DESIGN AND TEST EXPERIENCES WITH INSTABILITY OF MAJOR AIRFRAME COMPONENTS

By Walter E. Binz, Jr.

The Boeing Company
Transport Division

SUMMARY

Two test incidents involving instability of large scale commercially built structures are described. Two classes of structure are discussed; the first, a fuselage with skin designed to buckle at low stress, and the second, a wing whose surface remains unbuckled to failure. The structure in the region of failure is defined and the failures described and illustrated. Insofar as possible, the stresses in the critical area at the time of failure are reported and compared to strength determined by analysis. Both fuselage and wing surfaces were observed to fail in the mode of a medium range column when adequate support was provided by ribs and frames. Initial failure in the wing example was premature due to a design deficiency in rib strength. A clear illustration is given of the effect of rib stiffness on wing surface stability. Adding stiffness to wing ribs increases the limit of surface stability to the theoretical flat panel value.

INTRODUCTION

Tests of large, full scale, stiffened shell structures, built by production quality mechanics with production tools, rarely get attention in the technical literature. Individuals in the technical community have limited access to data from these types of tests. Investigators of structural stability have recognized that imperfections exist in all structures and have attempted to evaluate their effects on the limits of stability. The tested structures described in this report are imperfect to the degree which may be expected for commercially built airframes. These imperfections are not specifically defined but one might expect that their effect could be qualitatively evaluated by observing any marked deviation in the behavior of these structures from the theoretical or experimental behavior of near perfect specimens.

SYMBOLS

b	stiffener spacing, in.
b_e	effective width of skin between stringers, in.
c	coefficient of fixity in Euler column formula
D_1	plate flexural stiffness in longitudinal direction, in.-kips
D_2	plate flexural stiffness in circumferential direction,in.-kips
F	Young's modulus, ksi
E_1	plate extensional stiffness in longitudinal direction, kips/in.
h_e	average depth of wing box, in.
h_x	width of wing box, in.
I	moment of inertia of effective wing bending section, in.^{4}
K	buckling coefficient of flat plate, $\frac{\sigma_{cr} b^2}{\eta E t^2}$
ℓ	length of surface between frames or ribs, in.
M	spanwise wing bending moment, in.-lbs.
N_p	compressive load per inch at panel buckling, kips/in.
P	rib crushing load, lbs./in.
r	initial radius of curvature of wing, in.
R	radius of cylinder, in.
t	thickness of skin, in.
γ	empirical correction for initial imperfections
$\bar{\epsilon}$	unit shortening
η	plasticity reduction factor
ρ	radius of gyration, in.
σ_{edge}	edge stress corresponding to strain $\bar{\epsilon}$, ksi

σ_{cc} local crushing stress of effective section, ksi

σ_{cr} compressive stress at local buckling of skin, ksi

A FUSELAGE INSTABILITY PROBLEM

During the static test program of the KC-135 jet tanker, one instability type failure occurred in the fuselage monocoque structure. This failure, in the lower aft body under the stabilizer, is shown in Figure 1 at the instant of failure. The critical section was loaded by a combination of bending, vertical shear and a small amount of torsion.

The structure in the vicinity of the failure may be described as a single cell tapered shell, any section of which is made up of an upper radius and a lower radius separated by a flat segment at the sides. Longitudinal stiffening was provided by hat section stringers which were spaced at about seven inches. Stringers had an area of .23 square inches and a ρ = .475 in. The monocoque skin was .040 - 7075-T6 clad curved to a radius of 35 inches. Frames were connected to the upstanding legs of the hat section stringers and did not interrupt the stringer continuity. The frame forward of the failure area was a partial bulkhead. The frame aft was a formed .051 gage 7075-T6 Z section 2.44 inches deep. The frame spacing was 24 inches.

Loads were applied in small increments up to failure and instrumentation read at each increment. Compression wrinkles in the lower surface skin were noticed at about 50% of the failure load. At 95% of the failure load, these buckles were very sharp. All load systems had stabilized after the application of the final load, however, the fuselage collapsed before data could be recorded.

Failure was initiated in the skin-stringer panel midway between the frames described. An inside view of the fuselage after failure is shown in Figure 2. The frames appeared to be in good condition after failure with no indication of lateral permanent set.

A group of strain gages were located on the critical stiffener within inches of the point of failure initiation. An analysis of these gage readings indicates that at the time of failure, the average stress in the effective bending structure was -43,000 psi. The stress computed using the elementary flexure formula applied to the effective body bending section is also -43,000 psi.

Allowable Stress Computation

At the time of this design, allowable compressive stresses were computed by the Johnson Parabolic formula

$$\sigma_{edge} = \sigma_{cc} - \frac{\sigma_{cc}^2 \left(\frac{\ell}{\rho\sqrt{c}}\right)^2}{4\pi^2 E}$$

A limited amount of test data was used to substantiate this analysis. A fixity coefficient c = 1.0 was assumed and ℓ was taken as the frame spacing. The strengthening effect of the body curvature was neglected. The effective section was calculated using a width of skin

$$b_e = 1.7\, t \sqrt{\frac{E}{\sigma_{edge}}}$$

The proportions of the stiffener were such that local crippling could not occur below the compressive yield stress of the material. Therefore,

$$\sigma_{cc} = F_{cy} = 62{,}000 \text{ psi} .$$

Computation of the allowable compressive stress at the point of test failure using this method yielded $\sigma_{edge} = -41{,}200$ psi. When compared to the test conditions at failure, this analysis underestimated the surface strength by less than 5%.

An analysis of the critical section using the techniques described by Peterson, Whitley and Deaton in reference 1 was recently completed. Manipulating the flat panel portion of equation 3, reference 1

$$N_p = \frac{c\pi^2 D_1}{\ell^2} + \gamma \frac{2}{R} \sqrt{E_1 D_2}$$

and again assuming the fixity coefficient c = 1, the edge stress at panel buckling was calculated as $\sigma_{edge} = -43{,}000$ psi. Consideration of curvature in this analysis would raise the edge stress to -44,700 psi at panel buckling.

On the strength of these analyses the consideration that the structure behaves as a flat simply supported column appears to be reasonable for structures of these proportions loaded in compression only. The skin, being buckled at a low stress, looses its ability to stabilize the stiffeners by shell action and permits a column failure mode to be predominate. Where the skin between stiffeners is buckled by high shear loads combined with compression, a more sophisticated analysis must be undertaken to account for the interaction of the shear in the skin on the compressive strength of the surface.

A WING INSTABILITY PROBLEM

A wing instability failure was encountered during the static destruction test program of the B-52A airplane. Failure was initiated by instability of the inspar wing structure and resulted in complete collapse of the upper surface of the left hand wing. Failure occurred approximately 25 feet outboard from the side of the body (one-third span) as shown in Figure 3. The critical section of the wing was loaded by a combination of bending, shear and torsion.

The primary structure is a single-cell, two-spar, box beam of constant width and tapered depth. Upper and lower surfaces are cambered in the chord direction. In the failure area, the wing box is approximately ten feet wide with an average depth of 33 inches. Upper surface spanwise stiffening is provided by extruded "J" section stiffeners spaced at approximately 8.5 inches and supported by chordwise ribs spaced at 30 inches. Ribs are of a stiffened web construction and constitute a beam member between front and rear spars. Spanwise stringers are continuous with their outstanding flanges attached to the chords of the supporting ribs. All primary structure is fabricated from 7075-T6 aluminum material with the exception of rib webs which are 2024-T3 aluminum material. In the region of failure, the upper surface skin-stringer combination has an area of .5 square inches per inch of width and a radius of gyration of 1.0 inches.

Loads were applied in small increments and instrumentation data obtained at each load level. At 88% of failure load, the deflection indicators used to measure rib crushing began to show a nonlinear load-deflection relationship. Incremental loading was continued until a sudden and complete failure occurred. At the final load application, the structure collapsed before instrumentation data could be obtained.

Failure was initiated by crushing of the ribs with the simultaneous collapse of the upper compression material in the aft portion of the box. Internal damage in the area of primary failure is shown in Figure 4. From an analysis of the recorded data taken from strain gages located in the failure area, the average stress in the upper surface material was -45,000 psi at failure. The stresses calculated in the failure area by the elementary flexure formula average approximately -50,000 psi. It seems likely that the softness of the supporting ribs in the test structure caused some of the upper surface load to shift to the more lightly loaded structure in the forward part of the box, thereby explaining the discrepancy between the measured test stresses and the calculated stresses in the aft portion of the box. Unfortunately, no strain gages were located on the forward part of the wing to substantiate this argument.

Ribs are generally used as stiffening members in flexible wings to prevent the collapse of the surface material. Rib crushing loads are proportional to the curvature of the wing. Rib loads for the critical wing rib were computed according to the formula:

$$P = \frac{M\ell}{h_e h_x r} + \frac{M^2 \ell}{h_e h_x EI_x}$$

which includes the effect of initial surface curvature and primary wing bending curvature. The computed rib loads were 380 lbs per inch of surface width under the failure conditions. A subsequent test of the rib under crushing loads indicated an ultimate strength of 600 lbs per inch of surface width. Its spring rate was found to be 4,300 lbs per inch deflection per inch of surface width. Since the rib was the primary cause of failure, the foregoing formula obviously did not account for the total rib crushing load experienced in the test.

In attempting to discover the reason for this discrepancy, it was observed that the rib adjacent to the critical rib had a considerably higher extensional stiffness since it formed a fuel tank bulkhead. As a consequence, the upper surface curvature was higher than expected at the critical rib and lower at the adjacent stiffer rib. The opposite effect occurred at the lower surface. A subsequent analysis, accounting for the differences in rib stiffness and the shearing deformations in the ribs caused by the unbalanced crushing loads, showed that the upper surface crushing load at the critical rib was actually 610 lbs per inch of surface width for the failure condition. This is in close agreement with the tested ultimate strength of this rib and emphasizes the importance of including all secondary effects in rib stress analysis.

Allowable Stress Computation

Curves of allowable wing surface stress versus $\frac{\ell}{\rho \sqrt{c}}$ were established on the basis of a large amount of experimental data accumulated for this airplane as well as previous Boeing airplanes. Since the surface skins were required to remain unbuckled at ultimate load, these design curves were modified in the short column range according to the formula

$$\sigma_{cr} = K \eta E \left(\frac{t}{b}\right)^2$$

A buckling coefficient of 5.0 was used to account for the skin being continuous over the stringers, curvature of the surface, and torsional restraint provided the stringers by the ribs.

The allowable surface stress in the failure area was computed as -56,000 psi using these procedures and assuming a fixity coefficient c = 1.0. An analysis using the formula

$$N_p = \frac{c\pi^2 D_1}{\ell^2}$$

with a fixity coefficient c = 1.0 gives an allowable edge stress equal to -56,000 psi. Premature rib failure restricted the surface stress level to -45,000 psi. As a result of this failure, the rib was reinforced to an ultimate strength of 390 lbs per inch of surface width. In a subsequent test of the wing incorporating these rib changes, the upper surface material reached a stress level of -53,000 psi. A failure in another part of the wing prevented further load application and testing was discontinued.

In an attempt to further substantiate the strength of the upper surface, a separate test program was initiated. Several tests were made on portions of the upper surface, curved to the shape of the deflected wing and laterally supported on springs simulating rib flexibility. Destruction tests of these panels established that the surface allowable of the wing as originally tested was -54,000 psi, and that, after improving the rib stiffness, the surface allowable increased to -55,500 psi. Further increases in rib stiffness produced no major improvement in strength. Similar tests on initially straight specimens (without wing bending curvature) indicated no improvement in strength over specimens that were initially curved.

CONCLUDING REMARKS

In the example of fuselage instability, the structure did not fail in a mode typical of cylindrical shells but tended to behave in much the same manner as a column. This might be expected in the case where the skin is designed to buckle in compression at low applied loads. The curvature of the section seemed to have only a minor effect on its strength.

In both the wing and fuselage examples the fact that the ribs and frames were uniformly spaced and offered little resistance to rotation of the surface structure seemed to permit the surfaces to deform to the characteristic single half wave shape between supports in the manner of a simply supported column. This is evidenced by the fact that the fixity coefficient for simple supports yields an analysis which closely approximates the actual tested strength.

The wing program gives definite indication that there is an optimum amount of rib stiffness required to develop the full surface strength. The radius of curvature of the wing ($\sim$2000 inches) had no appreciable effect on the surface strength.

REFERENCES

1. Peterson, James P., Whitley, Ralph O., and Deaton, Jerry W.: Structural Behavior and Compressive Strength of Circular Cylinders with Longitudinal Stiffening. NASA TN D-1251, 1962.

Figure 1.- Fuselage instability failure.

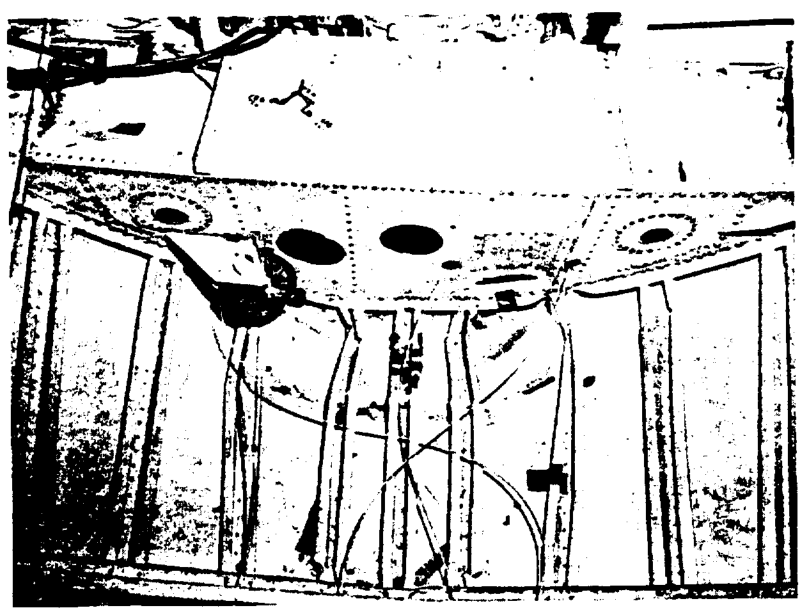

Figure 2.- Inside view - fuselage instability failure.

Figure 3.- Wing upper surface instability failure.

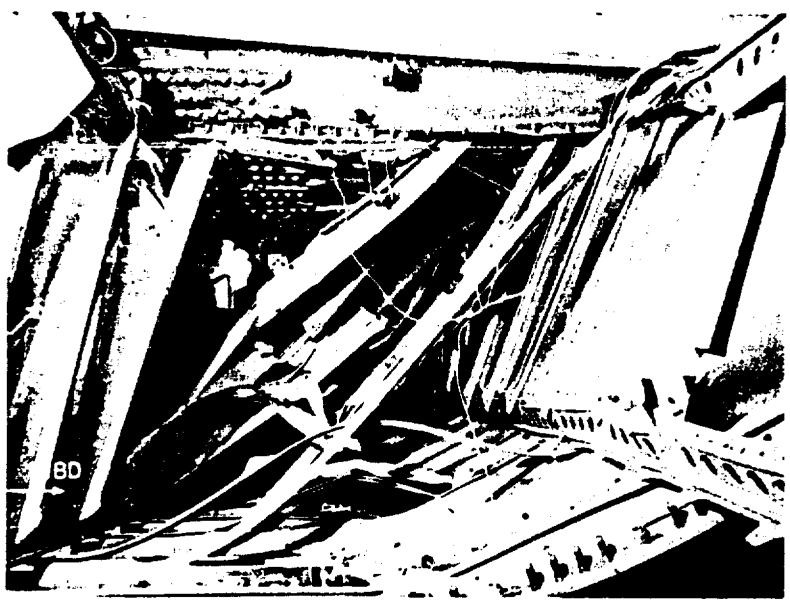

Figure 4.- Rear inside view - wing instability failure.

II CYLINDRICAL SHELLS